ACS APPLIED MATERIALS & INTERFACES

Research Article

www.acsami.org

A Universal Rule for Organic Ligand Exchange

Hongjun You,* Wenjin Wang, and Shengchun Yang*

MOE Key Laboratory for Non-equilibrium Synthesis and Modulation of Condensed Matter, State Key Laboratory for Mechanical Behavior of Materials, School of Science, Xi'an Jiaotong University, Xi'an, Shaanxi 710049, P. R. China

Supporting Information

ABSTRACT: Most synthetic routes to high-quality nanocrystals with tunable morphologies predominantly employ long hydro-carbon molecules as ligands, which are detrimental for electronic and catalytic applications. Here, a rule is found that the adsorption energy of an organic ligand is related to its carbon-chain length. Using the density functional theory method, the adsorption energies of some commonly used ligand molecules with different carbon-chain lengths are calculated, including carboxylate, hydroxyl, and amine molecules adsorbed on metal or metal oxide crystal surface. The results indicate that the adsorption energy of the ligand molecule with a long carbon chain is weaker than that of a smaller molecule with same functional group. This rule provides a theoretical support for a new kind of ligand exchange method in which large organic ligand molecules can be exchanged by small molecules with same functional group to improve the catalytic properties.

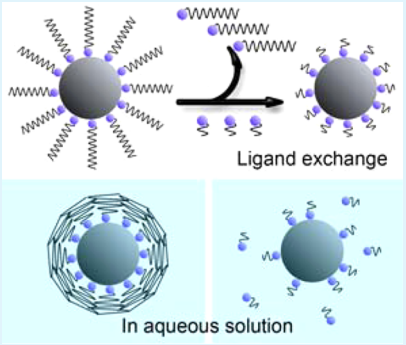

KEYWORDS: *surface treatment, adsorption energy, density functional theory, length of carbon chain, catalytic property*

INTRODUCTION

Applications of colloidal nanocrystals (NCs) with controlled shapes and sizes have been accompanied in many areas by a rapid increase in high-technical requirements, such as photoelectronics,[1−3] catalysis,[4−6] electronics,[7,8] magnetics,[9,10] biotechnology,[11,12] and surface-enhanced Raman spectroscopy.[13,14] In the shape-controlled synthetic routes for NCs, long hydrocarbon molecules (C_8 to C_{18}) with a coordinating headgroup, such as −COOH, $-NH_2$, and $-CH_2OH$, are generally required as ligands, which sterically stabilize NCs in nonpolar or hydrophobic solvents as well as play a key role in the shape control and self-assembly of NCs.[15,16] However, the presence of such bulky capping molecules is deleterious for NC applications because they can block chemicals or light from accessing the surfaces of NCs.[17−22] As confirmed by transmission electron microscopy (TEM) analysis in previous report, the longer alkyl chain led to a denser ligand shell on the NC surface and thus has effect on the penetrating of chemicals.[23]

In the past, much attention and effort have been devoted to the development of effective strategies that remove or exchange the ligand to reduce the inhibiting function of ligand to the catalytic properties. Thermal and oxidative approaches for removing the ligands, including the treatments with heat/calcination,[24] plasma,[25] high-temperature hydrogen,[26] UV−ozone,[27] and acid,[28] are not constantly effective because NCs become unstable at high temperature and oxidative condition.[29] For example, with the treatment of reflux hot water, poly(vinyl acetate) ligand on Au NC can be officially removed, while the size of NC slightly increased.[17] In a more recent report, the surface of Pd NC was poisoned by CO when poly(vinyl propylene) ligand was removed with UV−ozone, even though its morphology was maintained.[27]

The approach of ligand exchange in which the ligands are replaced with specifically designed species has drawn wide interests.[30,31] For example, Joanna Kolny-Olesiak and coworkers investigated the multiple ligand exchange process between oleic acid and pyridine on CdSe NC surface using nuclear magnetic resonance method.[32] Through ligand exchange, the NCs can be transferred from nonpolar solvent to polar solution, and their surface exposure also can be enhanced.[18] However, in the previous study, the ligand was exchanged by a new molecule with different and stronger adsorbent functional group, such as thiols,[21,33,34] hydrazine,[8] phenyldithiocarbamate (PTC),[35] $BF_4{\cdot}NO$,[18] metal chalcogenides,[19,36] and metal-free chalcogenides.[37] Although the solubility in polar solution and surface exposure of NC were enhanced after ligand exchange, the new ligand molecules with different and stronger adsorbent functional groups were more difficult to be removed in the application stage. Furthermore, the original surface states will be destroyed by the new and different adsorbed functional groups, such as surface sulfuration by thiol groups.

In our previous study, we tried a new ligand exchange method in which the butylamine (BAm) molecule was used to exchange oleylamine (OAm) ligand.[4,38,39] Different from previously reported ligand exchange, the exchanged ligand and exchanging ligand have the same functional group, namely, the amine group. After treatment, the catalytic properties of NCs were obviously activated. However, the theoretical rule behind this novel experimental phenomenon still has not been disclosed. Here, using the density functional theory (DFT)

Received: July 25, 2014
Accepted: October 22, 2014
Published: October 22, 2014

calculation, we find the adsorption of BAm molecules on metal NCs is stronger than that of the OAm molecules. This result can explain thermodynamically why the OAm ligands can be exchanged by BAm molecules. Furthermore, through a great deal of calculation, we find a universal and important rule. The adsorption energy of organic ligand is related to its carbon-chain length. For the organic ligand molecules with same functional group, the smaller molecule has stronger adsorption energy than the larger molecule. On the basis of this rule, a new kind of ligand exchange can be proposed in which the small organic molecules with same functional group can be used to exchange the large molecules with long carbon-chains. Compared with traditional ligand exchange method, this new kind of ligand exchange method has a great merit: after ligand exchange, the new ligands have the same functional group with original ligand. Thus, the morphology of NCs can be well-maintained, and the surface structure cannot be destroyed by the ligand exchange.

RESULTS AND DISCUSSION

Amine molecules with long carbon chains are very commonly used ligands in the synthesis of metal colloid NCs. The adsorption energies of amine molecules with different carbon-chain lengths adsorbed on metal surface are first calculated using the DFT method. The calculation process is similar to our previous report.[16] The structures of both metal crystal with periodical boundary and amine molecules are optimized before they are brought together. Then, the whole structure of amine molecules adsorbing on metal surface are fully optimized using the DFT method (details in Supporting Information). In this system, the carbon-chain lengths of amine molecules change from one carbon atom (C_1) to 16 carbon atoms (C_{16}). Figure 1

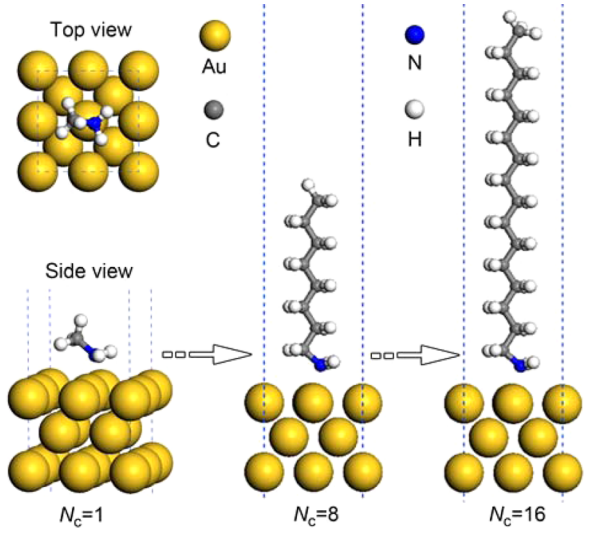

Figure 1. Optimized configurations of amine molecules adsorbed on Au (100) surface with different carbon-chain length in a periodic cell using DFT method. The carbon atoms (N_c) in the carbon chains increase from 1 to 16.

shows the representative optimized configurations of amine molecules with different lengths of carbon chains (numbers of carbon atoms (N_c) are 1, 8, and 16) adsorbed on Au (100) facet.

Figure 2 shows the electron density distribution when the amine molecules adsorbed on Au (100) facet. The amine group

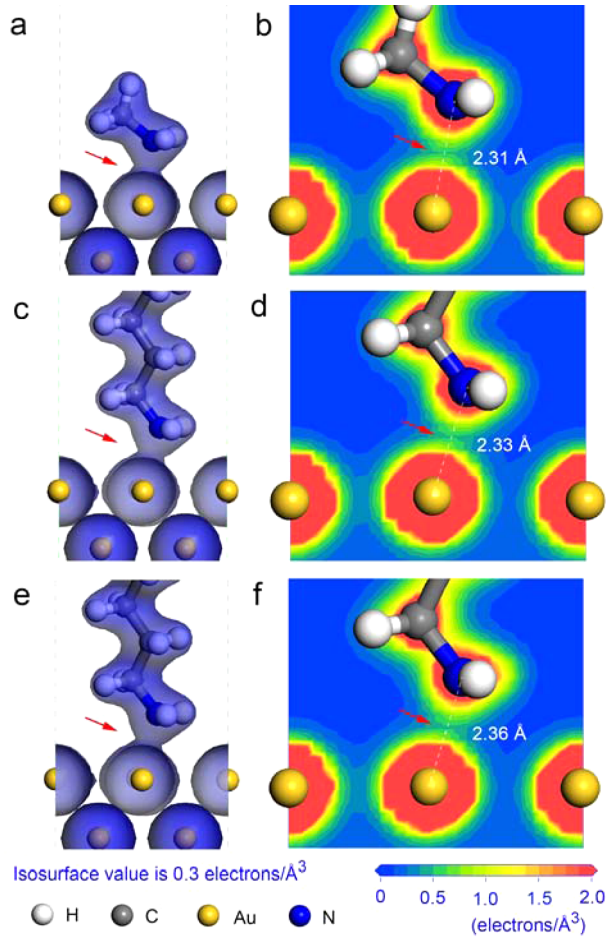

Figure 2. Distributions of electron density when amine molecules with different length of carbon chains adsorbed on Au (100) surface. The carbon-chain lengths are (a, b) 1, (c, d) 8, and (e, f) 16 carbon atoms. (a, c, e) The isosurfaces of electron density with value of 0.3 electrons/Å^3. (b, d, f) The center slices of electron density distributions.

adsorbs exclusively with a single metal atom at a top site on the metal surface via nitrogen atom. No other binding is found on all of the high-symmetry sites between the amine molecule and Au surface. This interaction structure between amine group and Au surface can be rationalized by the electron density distribution in the electron clouds formed between amine group and Au atom (Figure 2a–c). The center-slice maps of the electron density distribution (Figure 2d–f) show that Au atom connects N atoms along the top direction of the C–N–H_2 tetrahedron to form the maximum electron cloud overlap. The maximum coordination number of N atom is four, so the structure is the optimized configuration for the amine group adsorption on noble metal surface. With the carbon-chain length of the amine molecules increasing, the isosurface with a value of 0.3 electrons/Å^3 between N and Au atoms becomes narrow gradually (Figure 2a–c). The center-slice maps (Figure 2d–f) show that the electron densities between the N and Au atoms are decreased with the increase of the length of the carbon chains, accordingly. Simultaneously, the distance between the N and Au atoms increases from 2.31 to 2.33 Å and 2.36 Å as the carbon-chain length increases from 1 to 8 and 16 carbon atoms, respectively.

The adsorption energies (E_a) of amine molecules with different carbon-chain lengths adsorbed on the Au (100) facet (Figure 3a) show that the increase of carbon atoms in the

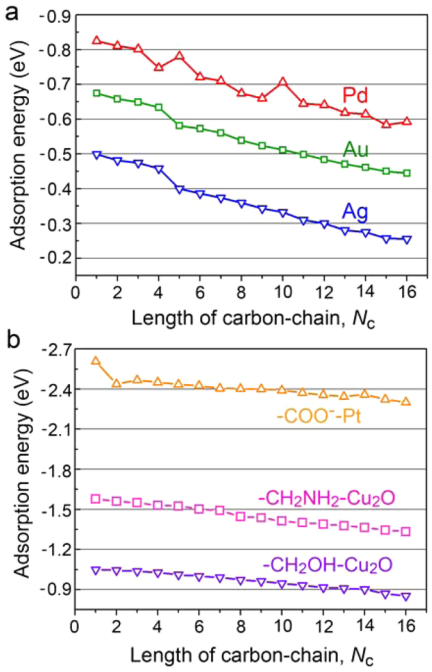

Figure 3. DFT-calculated adsorption energies of (a) amine molecules on Pd, Au, and Ag (100) surfaces, and (b) various organic ligand molecules with $-COO^-$ group adsorbed on Pt (100) surface ($-COO^-$–Pt), $-CH_2NH_2$ group adsorbed on Cu_2O (100) surface ($-CH_2NH_2$–Cu_2O), and $-CH_2OH$ group adsorbed on Cu_2O (100) surface ($-CH_2OH$-Cu_2O).

carbon chain (N_c) weakens the adsorption of molecules on the metal surface. Using the same DFT calculation method, the adsorptions of amine molecules on other metal surface, such as Ag (100) and Pd (100) planes, were also calculated. The configurations of amine molecules adsorbed on Ag (100) and Pd (100) facets are very similar to those on Au (100). As Figure 3a shows, the absolute value of adsorption energies ($|E_a|$) of amine molecules on Ag (100) and Pd (100) facets decreases gradually when the carbon-chain length (N_c) of amine molecules increases from one to 16. On the Pd (100) surface, the deviation of data is more obvious than that on Ag and Au surfaces, especially at N_c= 5 and 10 data points. The relationship between adsorption energy and carbon-chain length of amine molecules was further studied on different crystal facets. The configurations of amine molecules adsorbing on (100), (110), and (111), three low-index facets of Pt metal crystal, are similar to those on Au (100) facet. The amine group adsorbs exclusively with a single metal atom at a top site on the metal surface via its nitrogen atom. As shown in Supporting Information, Figure S1, on the Pt (100), (110), and (111) facets, the adsorption of amine molecules also becomes weaker with the increase of carbon-chain length.

Usually, the NCs are synthesized and applied in solution systems. Thus, the adsorption energies of amine molecules on Au (100) surface in three solution systems, namely, hexane, acetone, and ethanol solutions, are calculated using DFT method. As shown in Supporting Information, Figure S2, in the acetone solution, the configurations and electron density distributions of amine molecules adsorbed on Au (100) surface are similar to those in a vacuum system (Figure 2). The difference is the distance between N and Au atoms: it is a little less than that in the vacuum system. For example, the distance is changed from 2.31 to 2.27 Å for the methylamine adsorbed on the Au (100) surface. Supporting Information, Figure S3 shows the same with that in vacuum system; in hexane, acetone, and ethanol solutions, the adsorptions of amine molecules become stronger with metal surface when the carbon-chain lengths decrease from 16 to one carbon atom.

The relationship between adsorption energies and carbon-chain lengths of organic ligand molecules is further widely studied in other systems, not limited to pure metal surfaces and amine molecules. On the alloy crystal surfaces, such as Pt_3Cu, Pt_3Pd, and PtPd (100) facets, the adsorptions of amine molecules are calculated. As shown in Supporting Information, Figure S4a, on the (100) facet of Pt_3Cu alloy, Pt atoms show a stronger adsorption toward amine molecules than Cu atoms. For the Pt_3Pd (100) and PtPd (100) facets, the adsorption of amine molecules on Pd atom are stronger than that on Pt atom (Supporting Information, Figure S4b). As with the previous result, the absolute value of adsorption energies of amine molecules gradually decrease with the number of carbon atoms in carbon chain (N_c) increasing from one to 16 (Supporting Information, Figure S5). Besides alloy surfaces, the metal-oxide surface, such as Cu_2O (100) facet, is also investigated as the substrate for amine molecules adsorption. In addition, the adsorptions of other organic ligands with different functional groups, such as carboxylate ion group ($RCOO^-$) and hydroxyl group (RCH_2OH), are also calculated. Similarly, with these systems, including the carboxylate ion group ($RCOO^-$) on Pt (100) surface, the amine group (RCH_2NH_2) on cuprous oxide (Cu_2O) (100) surface, and the hydroxyl group (RCH_2OH) on Cu_2O (100) surface, as shown in Figure 3b, the adsorption energies of ligand molecules with different functional groups on different inorganic crystal surfaces show the same trend: the smaller molecules with the same functional group exhibit stronger adsorption energy than the larger molecules with longer carbon chains.

Double (C═C) and triple (C≡C) carbon bonds always exist in carbon chains of organic ligands, such as OAm molecule. The adsorption energies were calculated when one of the single bonds (C–C) in the hexadecylamine carbon chain was replaced by a double (C═C) or triple (C≡C) bond, as shown in Supporting Information, Figure S6. The absolute value of adsorption energy decreases dramatically when the first C–C bond near the amine group is replaced by a C═C or C≡C bond but has no obvious change when the other C–C bonds are replaced. This result indicates that the C═C or C≡C bonds have no obvious effects on the adsorption energy of amine molecules except when it is the first bond near the amine group.

All of the calculated systems support the same result that for the organic ligand with same functional group, the adsorption of a smaller molecule is stronger than that of a larger molecule. This universal and important rule has wide application in chemical synthesis and surface treatment of colloid NCs. Using this rule, a new kind of ligand exchange method can be proposed in the surface treatment of colloid NCs. Usually, in shape-controlled synthetic routes, the surface of the obtained NCs is densely covered by large organic molecules with long carbon chains. When the NC is applied in a polar solution, the long carbon chains of the organic ligand will be repelled by the polar solution and will thickly wrap the surface of NC (Figure 4b). Thus, the chemicals in the solution are blocked from accessing the surface of NC, resulting in greatly depressing catalysis or the sensing properties of NCs. According to this universal rule obtained from our calculation, the organic ligands

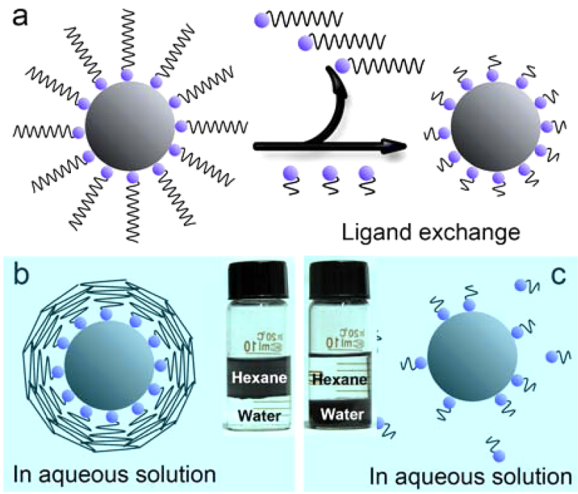

Figure 4. Schematic images of (a) ligand exchange between molecules with long and short carbon chains, (b) before and (c) after ligand exchange the NC states in aqueous solution. (b, inset) and (c, inset) Photographs of colloidal dispersions of amine-capped Pt blacks, showing that the BAm-capped Pt NCs are dispersed in the bottom water layer, and the OAm-capped Pt NCs are dispersed in the upper hexane layer.

with long carbon chain can be exchanged by corresponding small molecules with same functional group in thermodynamically favored ways, as shown in Figure 4a. Different than previous ligand exchange method, using this new kind of ligand exchange, the replacing molecules have the same functional group as those of the replaced molecules. After ligand exchange, the smaller adsorbed ligand molecules are soluble in polar solutions and thus can more easily be removed from the surface through dissolving into polar solutions due to their consistency with solutions (Figure 4c). During this kind of ligand exchange, the surface structures and morphology of NCs will not be changed by the new ligands because they have the same functional groups as the original ligand.

The insets of Figure 4b,c show the dispersion probability of Pt black in polar and nonpolar solutions when the Pt NPs in the Pt black were wrapped by OAm or BAm ligand. The Pt black adsorbed with OAm or BAm ligand was put into a bottle with 2 mL of water and 2 mL of hexane. After shaking for 2 min and then putting stable for 5 min, as shown in the insets of Figure 4b, the OAm-capped Pt black cannot be dispersed in water solution. By contrast, the BAm-capped Pt black can be well-dispersed in water solution (inset of Figure 4c). OAm and BAm have the same functional group, namely, the amine group, and just the lengths of carbon chains are different. OAm is one of the most commonly used ligands in the synthesis of NCs using organic method. On the basis of the universal rule we found in this paper, the OAm ligand, which has a long carbon chain, can be automatically exchanged by BAm ligand, which has a shorter carbon chain. After ligand exchange, the catalytic or sensing properties of NCs in polar solutions, such as water solution, should be greatly enhanced. In the following, the Pt_3Pd cubic NCs synthesized using OAm ligand are used to investigate the validity of this new kind of facile ligand exchange method.

Following Yang group's method, OAm-stabilized Pt_3Pd NC is synthesized in an organic solution.[40] As Supporting Information, Figure S7 shows, the obtained cubic Pt_3Pd NCs with edge length of 13.9 nm are bound by (100) facets. To be used as electrochemical catalyst, the Pt_3Pd NCs are loaded on the carbon black. The new kind of ligand exchange method proposed in this paper is used to treat the carbon black-supported Pt_3Pd NCs. The catalyst is dispersed in BAm solution with stirring for 3 d. The infrared (IR) spectra of the Pt_3Pd NCs before and after the ligand exchange are shown in Supporting Information, Figure S8. After ligand exchange, the change in the IR spectra was evident at the section from 600 to 1800 cm^{-1} (Supporting Information, Figure S8b). The IR spectra before ligand exchange were typically due to the adsorbed OAm molecules on the Pt_3Pd NC surface. The peaks at 1388 and 880 cm^{-1} can be attributed to the C═C bond and its adjacent C−H bond, respectively. These peaks almost disappeared after ligand exchange, indicating that most of the adsorbed OAm molecules on the Pt_3Pd NCs were replaced by BAm molecules (because BAm molecules do not have C═C bonds). Simultaneously, the spectrum peaks originally located at 1090 and 1059 cm^{-1} were shifted to 1168, 1102, and 1029 cm^{-1} after ligand exchange. These peaks can be attributed to the C−N bonds in amine molecules when they adsorb with metal NCs. There are two kinds of atoms on the (100) surface of Pt_3Pd NCs, namely, Pt and Pd. So, the IR spectrum for C−N bond shows two peaks when the amine molecules adsorbed with different atoms. After ligand exchange, the BAm ligand shows stronger adsorption energy; thus, the IR spectrum peaks for C−N bond were shifted to high level. The TEM images of the cubic Pt_3Pd NCs before and after ligand exchange are shown in Supporting Information, Figure S9, which indicates that the size and morphology of the NCs were well-maintained after the treatment.

Using measurement method similar to that of our previous report,[41] the electrocatalytic properties of Pt_3Pd NCs before and after ligand exchange for methanol oxidation reaction (MOR) were studied, as shown in Figure 5. The electrochemical active surface areas (ECSAs) of the cubic Pt_3Pd NCs were calculated by measuring the hydrogen adsorption from the cyclic voltammetry (CV) curves (Figure 5a). Before ligand exchange, the ECSA of Pt_3Pd NCs is only 10.4 m^2/g, which is much lower than the theoretically calculated surface area of the NCs (22.6 m^2/g) on the bases of their shape and size. After ligand exchange, the ECSA increased to 18.6 m^2/g, which is closer to the theoretical value. Considering the loading of the NCs on carbon black, part of the surface is covered by carbon black, and almost all of the NCs surface are clearly exposed after ligand exchange. Figure 5b shows electrocatalytic activity of the cubic Pt_3Pd NCs before and after ligand exchange for the MOR. Before ligand exchange, the activity of 5 μg of Pt_3Pd NCs catalyst is only 0.13 mA at the peak potential (0.58 V). After ligand exchange, the activity greatly increases to 0.97 mA at the peak potential (0.59 V) for the same amount of Pt_3Pd NCs catalyst under the same measurement conditions. This value is approximately 7.5 times higher than that before ligand exchange.

Before ligand exchange treatment, the surface of cubic Pt_3Pd NCs is adsorbed by OAm ligand, which is insoluble in water solution. Because of the inconsistency of OAm molecules in water, the carbon chains of OAm molecules will tightly wrap the surface of Pt_3Pd NCs to prevent the access of hydrogen (for CV) or methanol (for MOR) during the catalytic measurement. After ligand exchange, the OAm is replaced by BAm, which is soluble in water solution and has a short carbon chain. During the CV measurement, the BAm molecules will desorb from the surface of Pt_3Pd NCs to be dissolved in the aqueous solution or

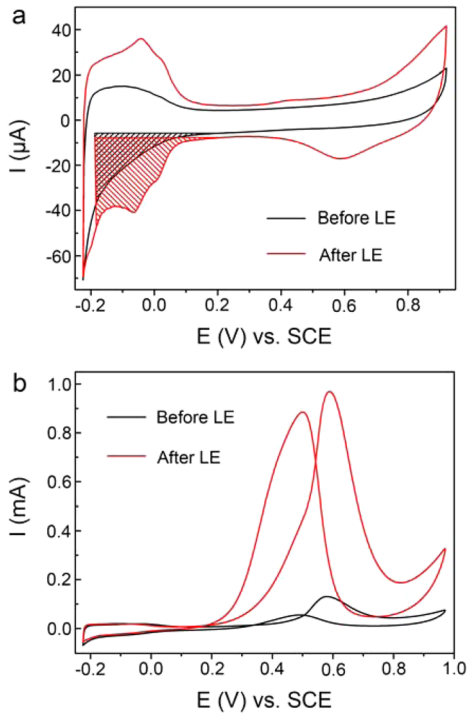

Figure 5. (a) The CV curves of Pt_3Pd NCs in the argon-saturated 0.1 M $HClO_4$ solution with 50 mV/s scan rate. The shaded areas indicate the hydrogen adsorption on the Pt_3Pd NCs before and after ligand exchange (LE) treatment. (b) The MOR curves catalyzed in a 0.1 M $HClO_4$ + 0.5 M MeOH aqueous solution.

be oxidized under high potential. Thus, the NC surface is cleaned, and its catalytic properties are greatly improved.

CONCLUSIONS

In summary, through using the DFT method to calculate the adsorption energies of organic ligand molecules with different carbon-chain lengths on metal or metal oxide crystal surface, a universal and important rule is found that small molecules have stronger adsorption energies than large molecules although they have the same functional group. On the basis of this rule, a new kind of ligand exchange is developed as the surface treatment method for colloid NCs: the large ligand molecules with long carbon chains can be replaced by the small molecules with the same functional group automatically in a thermodynamically favorable way. This new kind of treatment method will not change or destroy the original morphology and surface structure of the NCs because of the same functional groups possessed by the ligand molecules before and after ligand exchange. After ligand exchange, the smaller ligand molecules are soluble in polar solutions and thus can be more easily removed, inducing the increase of the catalytic properties of the NCs.

ASSOCIATED CONTENT

Supporting Information

DFT calculation method, experimental method, and supporting figures. This material is available free of charge via the Internet at http://pubs.acs.org.

AUTHOR INFORMATION

Corresponding Authors

*E-mail: hjyou@mail.xjtu.edu.cn. (H.Y.)

*E-mail: ysch1209@mail.xjtu.edu.cn. (S.Y.)

Notes

The authors declare no competing financial interest.

ACKNOWLEDGMENTS

This work is supported by the National Natural Science Foundation of China (Nos. 51201122 and 50901056) and the Doctoral Fund for New Teachers (No. 20120201120049).

REFERENCES

(1) McDonald, S. A.; Konstantatos, G.; Zhang, S. G.; Cyr, P. W.; Klem, E. J. D.; Levina, L.; Sargent, E. H. Solution-Processed Pbs Quantum Dot Infrared Photodetectors and Photovoltaics. *Nat. Mater.* **2005**, *4*, 138−142.

(2) Luther, J. M.; Law, M.; Beard, M. C.; Song, Q.; Reese, M. O.; Ellingson, R. J.; Nozik, A. J. Schottky Solar Cells Based on Colloidal Nanocrystal Films. *Nano Lett.* **2008**, *8*, 3488−3492.

(3) Gur, I.; Fromer, N. A.; Geier, M. L.; Alivisatos, A. P. Air-Stable All-Inorganic Nanocrystal Solar Cells Processed from Solution. *Science* **2005**, *310*, 462−465.

(4) You, H.; Peng, Z.; Wu, J.; Yang, H. Lattice Contracted Agpt Nanoparticles. *Chem. Commun.* **2011**, *47*, 12595−12597.

(5) Chen, A. C.; Holt-Hindle, P. Platinum-Based Nanostructured Materials: Synthesis, Properties, and Applications. *Chem. Rev.* **2010**, *110*, 3767−3804.

(6) You, H.; Yang, S.; Ding, B.; Yang, H. Synthesis of Colloidal Metal and Metal Alloy Nanoparticles for Electrochemical Energy Applications. *Chem. Soc. Rev.* **2013**, *42*, 2880−2904.

(7) Talapin, D. V.; Murray, C. B. Pbse Nanocrystal Solids for N- and P-Channel Thin Film Field-Effect Transistors. *Science* **2005**, *310*, 86−89.

(8) Hochbaum, A. I.; Chen, R. K.; Delgado, R. D.; Liang, W. J.; Garnett, E. C.; Najarian, M.; Majumdar, A.; Yang, P. D. Enhanced Thermoelectric Performance of Rough Silicon Nanowires. *Nature* **2008**, *451*, 163−167.

(9) Ge, J. P.; Lee, H.; He, L.; Kim, J.; Lu, Z. D.; Kim, H.; Goebl, J.; Kwon, S.; Yin, Y. D. Magnetochromatic Microspheres: Rotating Photonic Crystals. *J. Am. Chem. Soc.* **2009**, *131*, 15687−15694.

(10) Dong, A. G.; Chen, J.; Vora, P. M.; Kikkawa, J. M.; Murray, C. B. Binary Nanocrystal Superlattice Membranes Self-Assembled at the Liquid-Air Interface. *Nature* **2010**, *466*, 474−477.

(11) Smith, A. M.; Nie, S. M. Next-Generation Quantum Dots. *Nat. Biotechnol.* **2009**, *27*, 732−733.

(12) Wu, S. W.; Han, G.; Milliron, D. J.; Aloni, S.; Altoe, V.; Talapin, D. V.; Cohen, B. E.; Schuck, P. J. Non-Blinking and Photostable Upconverted Luminescence from Single Lanthanide-Doped Nanocrystals. *Proc. Natl. Acad. Sci. U.S.A.* **2009**, *106*, 10917−10921.

(13) You, H.; Ji, Y.; Wang, L.; Yang, S.; Yang, Z.; Fang, J.; Song, X.; Ding, B. Interface Synthesis of Gold Mesocrystals with Highly Roughened Surfaces for Surface-Enhanced Raman Spectroscopy. *J. Mater. Chem.* **2012**, *22*, 1998−2006.

(14) Yang, Z.; Zhang, L.; You, H.; Li, Z.; Fang, J. Particle-Arrayed Silver Mesocubes Synthesized Via Reducing Silver Oxide Mesocrystals for Surface-Enhanced Raman Spectroscopy. *Part. Part. Syst. Charact.* **2013**, *31*, 390−397.

(15) Talapin, D. V.; Lee, J. S.; Kovalenko, M. V.; Shevchenko, E. V. Prospects of Colloidal Nanocrystals for Electronic and Optoelectronic Applications. *Chem. Rev.* **2010**, *110*, 389−458.

(16) Peng, Z. M.; You, H. J.; Yang, H. Composition-Dependent Formation of Platinum Silver Nanowires. *ACS Nano* **2010**, *4*, 1501−1510.

(17) Lopez-Sanchez, J. A.; Dimitratos, N.; Hammond, C.; Brett, G. L.; Kesavan, L.; White, S.; Miedziak, P.; Tiruvalam, R.; Jenkins, R. L.; Carley, A. F.; Knight, D.; Kiely, C. J.; Hutchings, G. J. Facile Removal of Stabilizer-Ligands from Supported Gold Nanoparticles. *Nat. Chem.* **2011**, *3*, 551−556.

(18) Dong, A. G.; Ye, X. C.; Chen, J.; Kang, Y. J.; Gordon, T.; Kikkawa, J. M.; Murray, C. B. A Generalized Ligand-Exchange Strategy

Enabling Sequential Surface Functionalization of Colloidal Nanocrystals. *J. Am. Chem. Soc.* **2011**, *133*, 998−1006.
(19) Kovalenko, M. V.; Scheele, M.; Talapin, D. V. Colloidal Nanocrystals with Molecular Metal Chalcogenide Surface Ligands. *Science* **2009**, *324*, 1417−1420.
(20) Rodriguez, P.; Kwon, Y.; Koper, M. T. M. The Promoting Effect of Adsorbed Carbon Monoxide on the Oxidation of Alcohols on a Gold Catalyst. *Nat. Chem.* **2012**, *4*, 177−182.
(21) Zhang, H. T.; Hu, B.; Sun, L. F.; Hovden, R.; Wise, F. W.; Muller, D. A.; Robinson, R. D. Surfactant Ligand Removal and Rational Fabrication of Inorganically Connected Quantum Dots. *Nano Lett.* **2011**, *11*, 5356−5361.
(22) Konstantatos, G.; Howard, I.; Fischer, A.; Hoogland, S.; Clifford, J.; Klem, E.; Levina, L.; Sargent, E. H. Ultrasensitive Solution-Cast Quantum Dot Photodetectors. *Nature* **2006**, *442*, 180−183.
(23) Fenske, D.; Sonstrom, P.; Stover, J.; Wang, X. D.; Borchert, H.; Parisi, J.; Kolny-Olesiak, J.; Baumer, M.; Al-Shamery, K. Colloidally Prepared Pt Nanoparticles for Heterogeneous Gas-Phase Catalysis: Influence of Ligand Shell and Catalyst Loading on CO Oxidation Activity. *ChemCatChem* **2010**, *2*, 198−205.
(24) Yu, R.; Song, H.; Zhang, X. F.; Yang, P. D. Thermal Wetting of Platinum Nanocrystals on Silica Surface. *J. Phys. Chem. B* **2005**, *109*, 6940−6943.
(25) Gehl, B.; Fromsdorf, A.; Aleksandrovic, V.; Schmidt, T.; Pretorius, A.; Flege, J. I.; Bernstorff, S.; Rosenauer, A.; Falta, J.; Weller, H.; Baumer, M. Structural and Chemical Effects of Plasma Treatment on Close-Packed Colloidal Nanoparticle Layers. *Adv. Funct. Mater.* **2008**, *18*, 2398−2410.
(26) Lee, I.; Morales, R.; Albiter, M. A.; Zaera, F. Synthesis of Heterogeneous Catalysts with Well Shaped Platinum Particles to Control Reaction Selectivity. *Proc. Natl. Acad. Sci. U.S.A.* **2008**, *105*, 15241−15246.
(27) Crespo-Quesada, M.; Andanson, J. M.; Yarulin, A.; Lim, B.; Xia, Y. N.; Kiwi-Minsker, L. Uv-Ozone Cleaning of Supported Poly-(Vinylpyrrolidone)-Stabilized Palladium Nanocubes: Effect of Stabilizer Removal on Morphology and Catalytic Behavior. *Langmuir* **2011**, *27*, 7909−7916.
(28) Mazumder, V.; Sun, S. H. Oleylamine-Mediated Synthesis of Pd Nanoparticles for Catalytic Formic Acid Oxidation. *J. Am. Chem. Soc.* **2009**, *131*, 4588−4589.
(29) Law, M.; Luther, J. M.; Song, O.; Hughes, B. K.; Perkins, C. L.; Nozik, A. J. Structural, Optical, and Electrical Properties of Pbse Nanocrystal Solids Treated Thermally or with Simple Amines. *J. Am. Chem. Soc.* **2008**, *130*, 5974−5985.
(30) Yu, D.; Wang, C. J.; Guyot-Sionnest, P. N-Type Conducting Cdse Nanocrystal Solids. *Science* **2003**, *300*, 1277−1280.
(31) Tang, J.; Kemp, K. W.; Hoogland, S.; Jeong, K. S.; Liu, H.; Levina, L.; Furukawa, M.; Wang, X. H.; Debnath, R.; Cha, D. K.; Chou, K. W.; Fischer, A.; Amassian, A.; Asbury, J. B.; Sargent, E. H. Colloidal-Quantum-Dot Photovoltaics Using Atomic-Ligand Passivation. *Nat. Mater.* **2011**, *10*, 765−771.
(32) Lokteva, I.; Radychev, N.; Witt, F.; Borchert, H.; Parisi, J.; Kolny-Olesiak, J. Surface Treatment of CdSe Nanoparticles for Application in Hybrid Solar Cells: The Effect of Multiple Ligand Exchange with Pyridine. *J. Phys. Chem. C* **2010**, *114*, 12784−12791.
(33) Luther, J. M.; Law, M.; Song, Q.; Perkins, C. L.; Beard, M. C.; Nozik, A. J. Structural, Optical and Electrical Properties of Self-Assembled Films of Pbse Nanocrystals Treated with 1,2-Ethanedithiol. *ACS Nano* **2008**, *2*, 271−280.
(34) Dubois, F.; Mahler, B.; Dubertret, B.; Doris, E.; Mioskowski, C. A Versatile Strategy for Quantum Dot Ligand Exchange. *J. Am. Chem. Soc.* **2007**, *129*, 482−483.
(35) Frederick, M. T.; Amin, V. A.; Cass, L. C.; Weiss, E. A. A Molecule to Detect and Perturb the Confinement of Charge Carriers in Quantum Dots. *Nano Lett.* **2011**, *11*, 5455−5460.
(36) Lee, J. S.; Kovalenko, M. V.; Huang, J.; Chung, D. S.; Talapin, D. V. Band-Like Transport, High Electron Mobility and High Photoconductivity in All-Inorganic Nanocrystal Arrays. *Nat. Nanotechnol.* **2011**, *6*, 348−352.
(37) Nag, A.; Kovalenko, M. V.; Lee, J. S.; Liu, W. Y.; Spokoyny, B.; Talapin, D. V. Metal-Free Inorganic Ligands for Colloidal Nanocrystals: S(2-), Hs(−), Se(2-), Hse(−), Te(2-), Hte(−), Tes(3)(2-), Oh(−), and Nh(2)(−) as Surface Ligands. *J. Am. Chem. Soc.* **2011**, *133*, 10612−10620.
(38) Wu, J. B.; Qi, L.; You, H. J.; Gross, A.; Li, J.; Yang, H. Icosahedral Platinum Alloy Nanocrystals with Enhanced Electrocatalytic Activities. *J. Am. Chem. Soc.* **2012**, *134*, 11880−11883.
(39) Wu, J. B.; Zhang, J. L.; Peng, Z. M.; Yang, S. C.; Wagner, F. T.; Yang, H. Truncated Octahedral Pt3ni Oxygen Reduction Reaction Electrocatalysts. *J. Am. Chem. Soc.* **2010**, *132*, 4984−4985.
(40) Wu, J.; Gross, A.; Yang, H. Shape and Composition-Controlled Platinum Alloy Nanocrystals Using Carbon Monoxide as Reducing Agent. *Nano Lett.* **2011**, *11*, 798−802.
(41) Peng, Z. M.; You, H. J.; Wu, J. B.; Yang, H. Electrochemical Synthesis and Catalytic Property of Sub-10 Nm Platinum Cubic Nanoboxes. *Nano Lett.* **2010**, *10*, 1492−1496.